

## SANDIA NATIONAL LABORATORIES HYDROGEN STORAGE DEVELOPMENT PROGRAM

### QUARTERLY PROGRESS REPORT FOR OCTOBER – DECEMBER 2010.

Sandia National Laboratories is a multi-program laboratory managed and operated by Sandia Corporation, a wholly owned subsidiary of Lockheed Martin Corporation, for the U.S. Department of Energy's National Nuclear Security Administration under contract DE-AC04-94AL85000.

#### ***TASK 1 – IEA/IPHE PARTICIPATION***

##### ***TASK 1.1 Hydrogen Storage Materials:***

Principal Investigator: Mark Allendorf

No participation this quarter.

#### ***TASK 2 – TUNABLE THERMODYNAMICS AND KINETICS FOR HYDROGEN STORAGE***

Principal Investigator: Mark Allendorf

##### ***TASK 2.1 NANOPARTICLE SYNTHESIS***

###### ***Subtask 2.1.1 MOF templates (SNL)***

*Melt infiltration of MOF templates.* Melt infiltration of various templates is reported in the literature and results in higher hydride loadings than we observe using solution methods. We performed several infiltration experiments this quarter to determine if MOFs are stable when exposed to molten hydride and if infiltration of the nanopores occurs. Two frameworks were used: Cu-BTC, a carboxylate-copper MOF that has 1.3 nm enclosed pores, and the magnesium version of MOF-74, which has one-dimensional 1.6-nm channels (Fig. 1). These were subjected to a “hot sintering” method to infiltrate with NaAlH<sub>4</sub> as follows:

- MOF + 10wt% NaAlH<sub>4</sub> + H<sub>2</sub>
- MOF and hydride mixed in the glove-box
- Sample exposed to hydrogen pressure at room temperature
- Increase temperature to 195 °C and hold for 90 minutes

Under these conditions Cu-BTC is reduced to copper metal, as indicated by powder XRD. However, MOF-74-Mg survives, as seen from the PXRD in Figure 2. FTIR indicates that the hydride is present in the sample and the lack of peaks corresponding to bulk NaAlH<sub>4</sub> in the PXRD in Figure 2 indicates that the hydride is within the pores and not merely coating the outside of the particles. Additional characterization, elemental analysis, and hydrogen desorption experiments will be conducted next quarter to quantify the loading and determine the effects of confinement on the hydride.

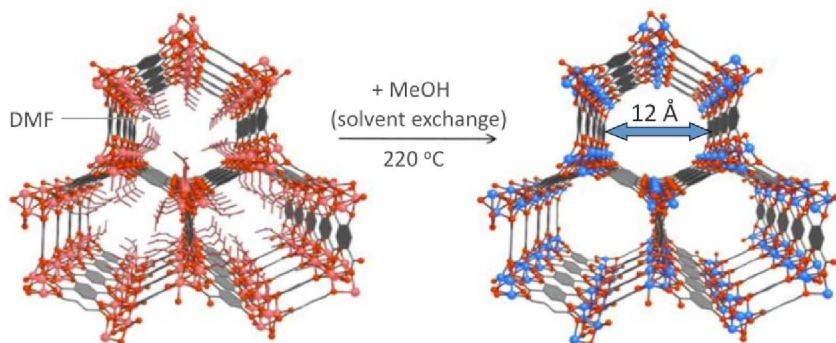


**Figure 1.** Pore structure and dimensions of MOF-74, illustrating the removal of coordinated solvent following synthesis.

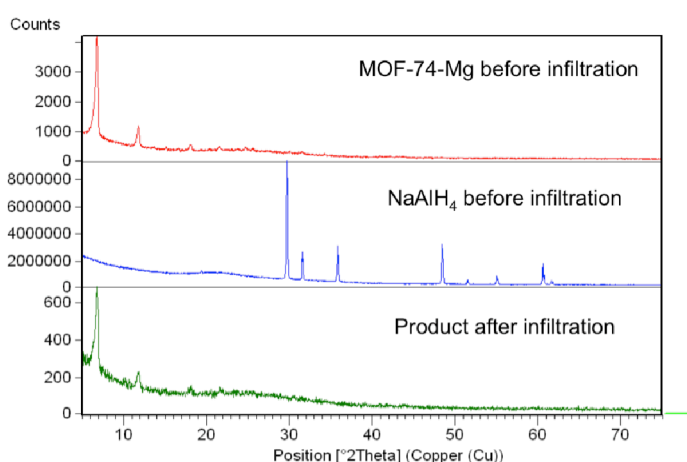


**Figure 2.** Powder x-ray diffraction of MOF-74, showing that the MOF is intact following melt infiltration. The absence of peaks corresponding to bulk hydride after infiltration confirms that the hydride, which is detected by FTIR spectroscopy, is located within the pores.

## **TASK 2.2 HYDROGEN SORPTION MEASUREMENTS AND KINETICS**

### *NaAlH4@Cu-BTC MOF H2 desorption (Sandia and UMSL)*

During the first year of this project we showed that infiltration of NaAlH<sub>4</sub> into the 1.3-nm pores of Cu-BTC results in an acceleration of the H<sub>2</sub> desorption kinetics. However, we did not have sufficient data to determine if the thermodynamics were altered by confinement as well. This quarter we completed new desorption experiments using the Simultaneous Thermogravimetric Molecular Beam Mass Spectrometry (STMBMS) instrument at Sandia. These results, in conjunction with computational modeling, strongly suggest that these particles are thermodynamically as well as kinetically destabilized relative to bulk. Two changes were made to obtain more readily interpretable data: the aperture size was decreased to 11 μm, thereby increasing the gas pressure in the cell; the reaction was initiated at a lower temperature (110 °C), so that the kinetics of only the initiation reaction(s) would be observed; and smaller temperature steps were taken (5 – 10 °C) to avoid high temperatures that would promote nucleation of bulk

material and melting. Using this approach, we obtain two smooth desorption profiles (Fig. 3) corresponding to the two-step decomposition of  $\text{NaAlH}_4$ . The activation energy measured for  $\text{H}_2$  desorption is  $\sim 86$  kJ/mol, in good agreement with the literature (W. Luo, K.J. Gross/*J. Alloys Compounds* 385 (2004) 224).

Hydrogen desorption from  $\text{NaAlH}_4$ -infiltrated Cu-BTC MOF displays very different behavior from the bulk materials, as seen in Fig. 4. At the lowest temperatures ( $110$  –  $130$  °C) quasi-equilibrium behavior is observed, but this corresponds to a very small amount of  $\text{H}_2$  loss, as seen in Fig. 4. Between  $130$  and  $165$  °C, a large  $\text{H}_2$  loss occurs, corresponding to a reduction in stoichiometry to  $\sim \text{NaAlH}_{3.2}$ . Here, the rate of desorption peaks initially and then decays (Fig. 4, left), which is characteristic of a diffusion mechanism. The corresponding activation energy is  $51$  kJ/mol  $\text{H}_2$ .

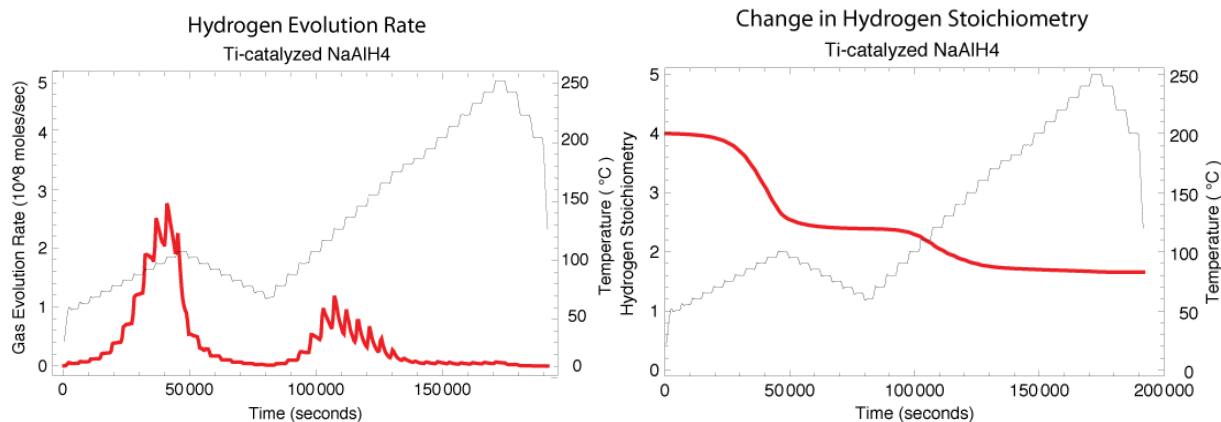


**Figure 3.** STMBMS data for Ti-catalyzed  $\text{NaAlH}_4$ . Left:  $\text{H}_2$  evolution rate; right: change in hydrogen stoichiometry.

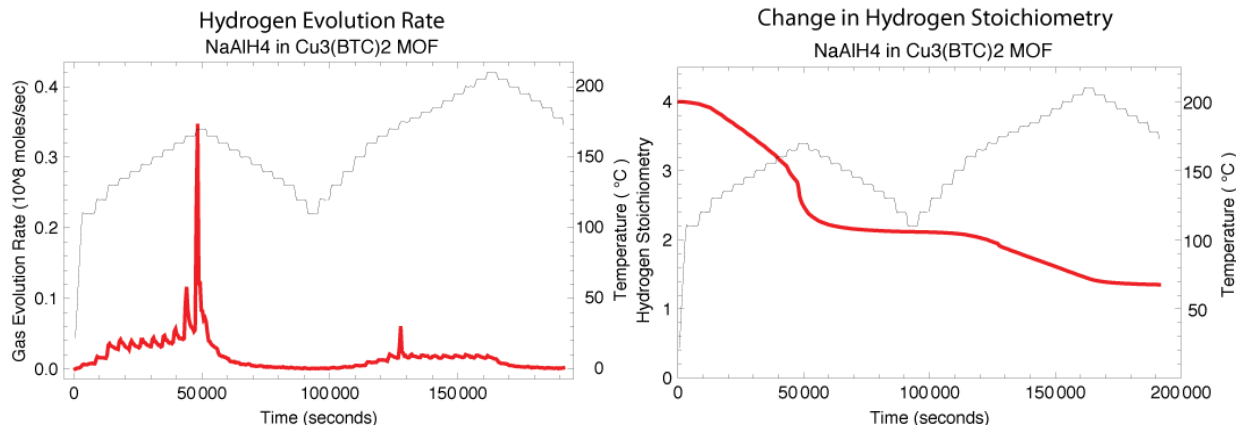
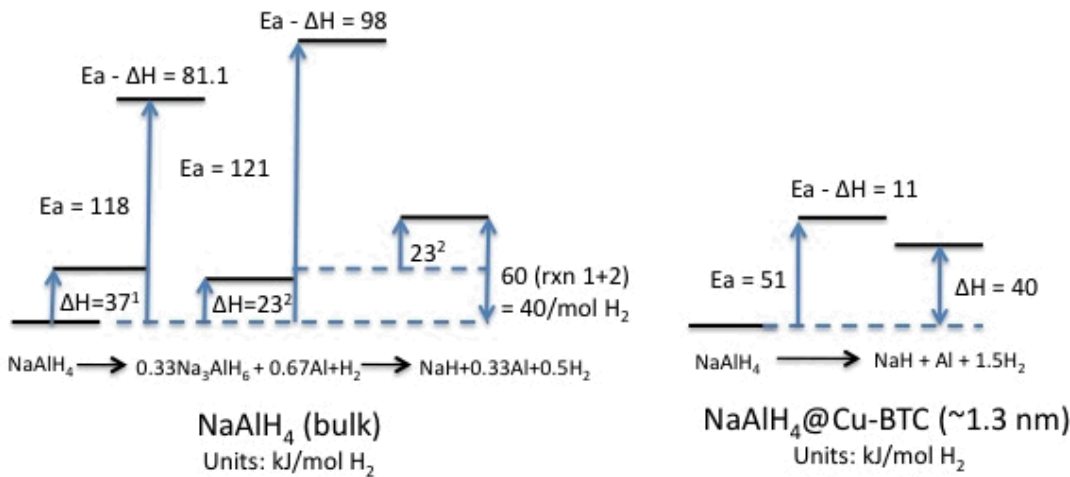


**Figure 4 (left).** STMBMS data for  $\text{NaAlH}_4$ @Cu-BTC. Left:  $\text{H}_2$  evolution rate; right: change in hydrogen stoichiometry.

These results are most easily understood by referring to an energy diagram (Fig. 5). For an endothermic reaction the activation energy includes both kinetic and thermodynamic components, as indicated by the energy level diagram in Figure 5. The left side of this diagram show the energetic picture for bulk  $\text{NaAlH}_4$ , while the right side shows the results obtained from

the STMBMS experiments. Clearly, if  $E_a$  measured for  $\text{NaAlH}_4@\text{Cu-BTC}$  is less than  $\Delta H^\circ(\text{bulk})$ , the thermodynamics of the hydride nanoparticles are altered by the confinement, with the nanoparticles being less stable than the bulk. This is not quite the case for  $\text{NaAlH}_4@\text{Cu-BTC}$ , for which we obtain  $E_a = 51 \text{ kJ/mol}$ , compared with  $\Delta H^\circ(\text{bulk}) = 37 \text{ kJ/mol H}_2$  for the reaction  $\text{NaAlH}_4 \rightarrow 0.33\text{Na}_3\text{AlH}_6 + 0.67\text{Al} + \text{H}_2$ . In contrast,  $E_a = 120 \text{ kJ/mol H}_2$  for the first step in bulk hydride decomposition, implying, at a minimum, that an enormous reduction of the activation barrier has occurred. Since, however, both experiments and theory in the literature indicate that  $\text{NaAlH}_4$  nanoclusters should decompose in a single step (e.g., see Mueller and Ceder, *ACS Nano*, 2010 and Lohstroh et al. *ChemPhysChem* 11 (2010), 789), without forming the intermediate hexahydride  $\text{Na}_3\text{AlH}_6$ , the STMBMS activation energy should actually be compared with  $\Delta H^\circ(\text{bulk})$  for the single-step reaction  $\text{NaAlH}_4 \rightarrow \text{NaH} + \text{Al} + 1.5\text{H}_2$ , which is  $40 \text{ kJ/mol H}_2$ . This indicates that the kinetic component of the nanoparticle activation energy is only  $11 \text{ kJ/mol}$ , assuming  $\Delta H^\circ$  is unchanged from the bulk. Since DFT calculations we performed for  $\text{NaAlH}_4$  cluster sizes of 2 – 8 formula units to indicate that the structure of these particles is quite different from the bulk, it is highly unlikely that  $\Delta H^\circ(\text{NaAlH}_4@\text{Cu-BTC})$  is the same as the bulk. Therefore, although individually these computational and experimental results are not definitive, together they present a strong case that  $\text{NaAlH}_4$  nanoclusters are destabilized in the 1 – 2 nm range, as is the case with Cu-BTC as a template. We note, however, that some ambiguity remains, because the work of Lohstroh et al. referenced above suggests that their particles are somewhat stabilized by their confinement in a porous carbon with a distribution of pore sizes (0.5 – 4 nm). Next quarter we will perform experiments using infiltrated MOF templates with larger pores (2.0 – 2.7 nm, MOF-74 and a UiO MOF) and will obtain H<sub>2</sub> desorption data for comparison with these results.



<sup>1</sup>Reaction 1: (uncatalyzed; Bogdanovic 2000):  $\text{NaAlH}_4 \rightarrow 0.33\text{Na}_3\text{AlH}_6 + 0.67\text{Al} + \text{H}_2$

<sup>2</sup>Reaction 2: (uncatalyzed; Bogdanovic 2000):  $0.33\text{Na}_3\text{AlH}_6 \rightarrow \text{NaH} + 0.33\text{Al} + 0.5\text{H}_2$

**Figure 5.** Left: energies of bulk  $\text{NaAlH}_4$  decomposition, which occurs by the two reactions indicated in the figure. Right: measured activation energy for  $\text{NaAlH}_4$ -infiltrated Cu-BTC.

*Gas evolution from  $\text{LiBH}_4@\text{hexagonal porous carbon}$ .* The calorimetry, H<sub>2</sub> release and uptake behavior, and the emission of toxic B<sub>2</sub>H<sub>6</sub> have been investigated in the desorption of LiBH<sub>4</sub>

confined in several pore-size carbon aerogel and highly-ordered nanoporous carbon templates. In contrast to the  $\text{LiBH}_4$  in carbon aerogels (CA-9 nm and CA-15 nm)  $\text{LiBH}_4$  confined in the highly ordered NPC (NPC-2 nm and NPC-4 nm) did not show Bragg peaks of the crystallized  $\text{LiBH}_4$ , the structural or melting transition (Fig. 6), due to the smaller pore size and subsequently induced amorphization. Nanoconfined  $\text{LiBH}_4$  desorbs hydrogen at a much lower temperature with respect to bulk  $\text{LiBH}_4$  (Fig. 7) and the dehydrogenation temperature decreases monotonically with the reduction of pore size. The reversibility of  $\text{LiBH}_4$  was demonstrated at 60 bar  $\text{H}_2$  and 250°C, and may be slowly reversible under even more moderate conditions. Most importantly, mass spectroscopic analysis indicates nanoconfinement can suppress or eliminate diborane release, implying that the reaction pathway leading to higher borane species by decomposing borohydrides may be controlled. This represents a major breakthrough in the reversibility of borohydrides for hydrogen storage, as the formation of very stable closoborane species, such as  $\text{B}_{12}\text{H}_{12}$  salts may be interrupted, and removed from the reaction pathway, opening the door to light-weight, reversible, boron-based hydrogen storage systems.

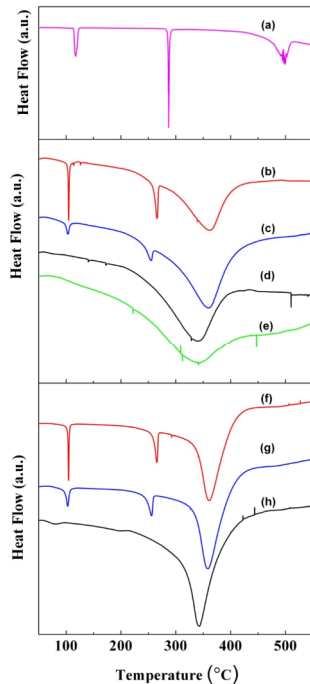


**Figure 6.** DSC plots of bulk  $\text{LiBH}_4$  and nanoconfined  $\text{LiBH}_4@\text{NPC}$  or  $\text{LiBH}_4@\text{CA}$ : (a) bulk  $\text{LiBH}_4$ ; (b)  $\text{LiBH}_4@\text{CA-15nm}$  with a loading of 10 wt%; (c)  $\text{LiBH}_4@\text{CA-9nm}$  with a loading of 10 wt%; (d)  $\text{LiBH}_4@\text{NPC-4nm}$  with a loading of 10 wt%; (e)  $\text{LiBH}_4@\text{NPC-2nm}$  with a loading of 10 wt%; (f)  $\text{LiBH}_4@\text{CA-15nm}$  with a loading of 20 wt%; (g)  $\text{LiBH}_4@\text{CA-9nm}$  with a loading of 20 wt%; (h)  $\text{LiBH}_4@\text{NPC-4nm}$  with a loading of 20 wt%.

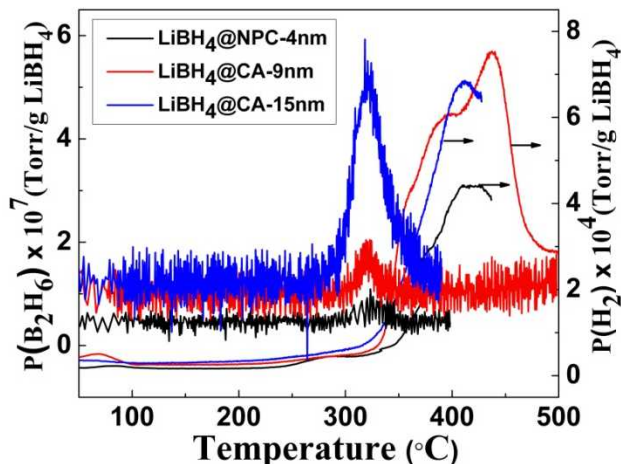


**Figure 7.**  $\text{B}_2\text{H}_6$  and  $\text{H}_2$  release with increasing temperature for  $\text{LiBH}_4@\text{NPC-4nm}$ ,  $\text{LiBH}_4@\text{CA-9nm}$ , and  $\text{LiBH}_4@\text{CA-15nm}$ . The loading of each sample is 10 wt%.

### **TASK 2.3 THEORETICAL MODELING FOR RATIONAL DESIGN OF PARTICLES**

#### *Subtask 2.3.1 (UMSL)*

*Phase diagram of nanocluster  $\text{NaAlH}_4$  from first-principles DFT.* We completed a first-principles calculation of the desorption pathway of nanocluster  $\text{NaAlH}_4$  into mixed metal NaAl nanoclusters. The decomposition is predicted to occur in a single step for a Na:Al ratio of 1:1, and contains no  $\text{Na}_3\text{AlH}_6$  intermediate due to the instability of the hexahydride anion from a Jahn-Teller distortion present in small clusters. The absence of hexahydride in the decomposition pathway is in agreement with  $\text{NaAlH}_4$ -infiltrated nanoporous carbon desorption experiments in the literature. Small clusters of aluminum hydride are predicted to be inherently stable, with increasing stability as the cluster size decreases with an enthalpy of 50-160 kJ/mol  $\text{H}_2$ . Our results further suggest that rehydriding of Al may be accomplished reversibly at relatively mild conditions if the particle size is restricted. With a suitable choice of framework, it may be possible to avoid the complicated wet chemical methods for recycling spent  $\text{AlH}_3$ . One to two formula units of NaH are predicted to spontaneously decompose and those above 3 formula units show no destabilization with an enthalpy around 70 kJ/mol  $\text{H}_2$ . Clusters of  $\text{NaAlH}_4$  show increased stability with decreasing size with a range of enthalpies of about 80-150 kJ/mol  $\text{H}_2$ . We also predict destabilized low-enthalpy reactions between simple metal hydride ( $\text{AlH}_3$  and NaH) and sodium alanate nanoclusters, which offer a potential way of tuning reaction thermodynamics using finite size effects.

This work is now in press in *J. Phys. Chem. C*.

#### *Subtasks 4.3.2 and 4.3.3 (MIT)*

*High-accuracy predictions of Li, Mg, Al, and alloyed MgAl hydride energetics.* This quarter we performed highly accurate calculations to evaluate the theoretical possibility of using the size of

nanoparticles to control the desorption energetics of hydrogen. This reaction focuses on the enthalpy difference as follows.

$$\Delta H = [E_{\text{metal}} + (n_{\text{H}}/2) E_{\text{H}_2} - E_{\text{hyd}}]/(n_{\text{H}}/2) \quad (1)$$

Our results thus far do not include thermal or zero-point contributions to the enthalpy. We find, however, that these contributions only shift the enthalpy relative to the total energy, so the changes in enthalpy are directly related to the changes in total energy. A full evaluation of these contributions to enthalpy is currently in progress.

In this quarter's work, endeavored to resolve two major questions: 1) What are the theoretical approximations in our calculation of energy differences; 2) how can we control the dependence of energy on size? Both these questions rely on evaluating energy differences accurately, and so we employed the following methodology. First, we perform highly accurate quantum simulations of the electrons using as a final test the quantum Monte Carlo method, as implemented in the QWalk package. We then compared these results to density functional theory predictions (Burkatski-Filippi-Dolg pseudopotentials with a QZP basis for Mg and Al, and full treatment of the core electrons with the Dunning quadruple zeta correlation consistent basis for Li and H). The arrangement of atoms when clusters are very small can be very different from the bulk, so we invested considerable time to finding minimum-energy geometries. Representative examples are given in Fig 8. Hydride geometries were determined using the Wang-Landau search method from Eric Mazjoub, and for the metallic clusters, where we could not find a reliable potential, we used a random search to locate a good approximation to the lowest-energy geometries. We sampled several relevant compositions, including Li, Mg, Al, and a 50/50 alloy of Mg and Al to investigate the effect of alloying at small system sizes. Clusters containing up to 18 metal atoms were included in the investigation, which corresponds to a particle radius of around 2 nm.

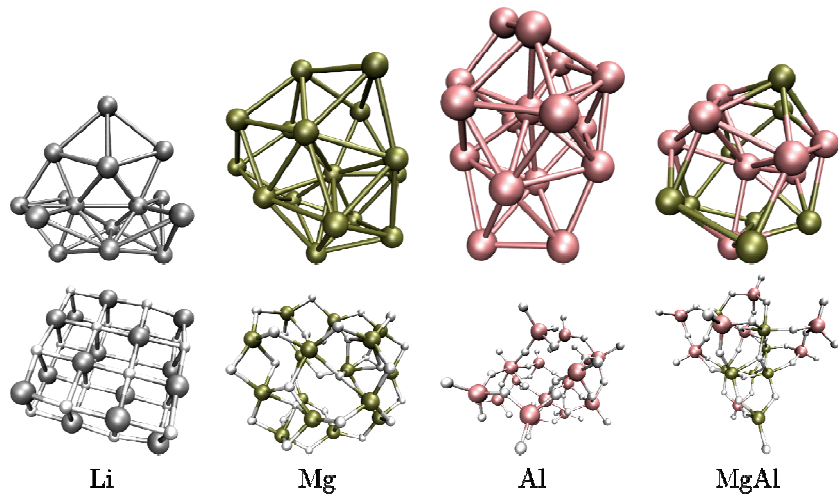


**Figure 8.** Examples of cluster geometries: 16 metal atoms.

Energies computed by diffusion Monte Carlo, using the trial nodal surface and minimum energy geometry from DFT(B3LYP) orbitals, are very slightly better (lower in energy) than the energies obtained from DFT(PBE) or Hartree-Fock. As seen in Fig 9, the hydride energy at small cluster sizes varies considerably among the different materials, and is the most significant contributor to the variation among the  $\Delta H$  results in shown in Fig 10. For larger sizes, which are comparable to

those produced experimentally in this project, the difference in slope between the pure metal and hydride determine the long-term characteristics.

Most of the curves in Fig. 10 have a very high derivative at small sizes, then saturate quickly to an almost zero slope. Although the individual binding energies are still changing significantly, as seen in Fig. 9, the slopes of the hydride and pure metal curves are almost identical, indicating that hydrogen binding energy changes very little in this size range. Only the MgAl alloy and perhaps the Al hydride have a non-zero slope at larger cluster size. Importantly, the results for MgAl clusters indicate that the dehydrogenation energy ( $\Delta H$ ) is approaching the desired range for hydrogen storage applications, particularly when an approximately 10 kJ/mol correction for zero point energy effects is included. *Furthermore, the values are intermediate between  $(Mg)_n$  and  $(Al)_n$ , supporting an original hypothesis of this project that form mixed-metal clusters of this type will moderate the thermodynamic behavior of  $MgH_2$  and  $AlH_3$ , leading to a hydrogen storage material more suitable for vehicular use than either of the two individual hydrides.*

We also validated our results versus experimental results on the bulk systems and the "gold standard" quantum chemistry method CCSD(T) and find excellent agreement. With results of this accuracy, we are also in a position to evaluate the quality of DFT predictions, which are typically used to guide hydride material discovery. The errors are summarized in Fig 11. The DFT results are scattered over a large range, and it is not completely clear which functional is the most reliable. Some functionals, such as the hybrid M06, have problems with particular materials, such as the Li clusters, but other functionals (e.g. PBE) appear to have errors that are more random.

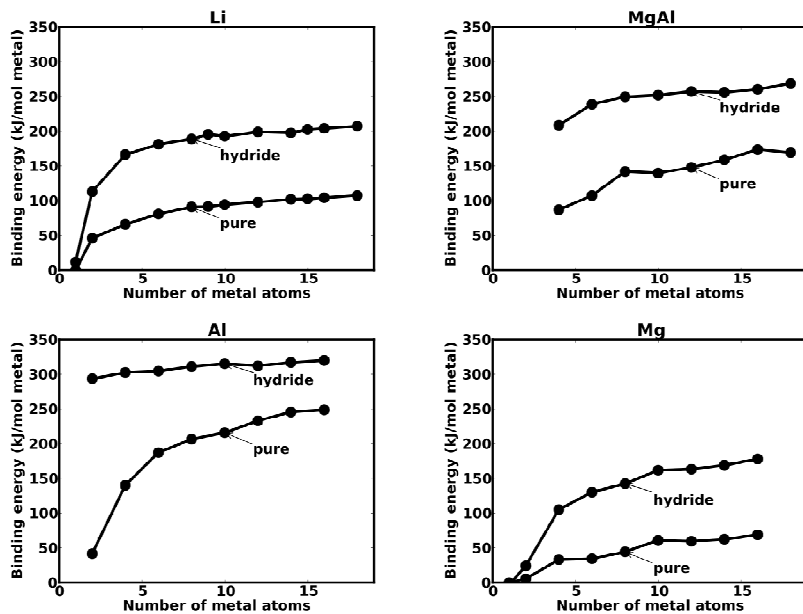


**Figure 9.** Hydride binding energies referenced to  $H_2$  and the pure metal, as calculated by diffusion Monte Carlo. The quantity  $\Delta H$  is proportional to the difference between these two curves.

In conclusion, we performed high accuracy calculations on nanoclusters of Li, Mg, Al, and alloyed MgAl hydrides to obtain the hydrogen desorption energy. We find that by alloying Mg with Al, we can interpolate between their behaviors and obtain nanoparticles with more attractive properties. We also find that lower-accuracy calculations such as DFT are not sufficient to properly predict the energetics of dehydrogenation. The results reconfirm our earlier conclusion that DFT calculations alone cannot be relied upon to accurately predict trends in nanoscale hydride stabilities.

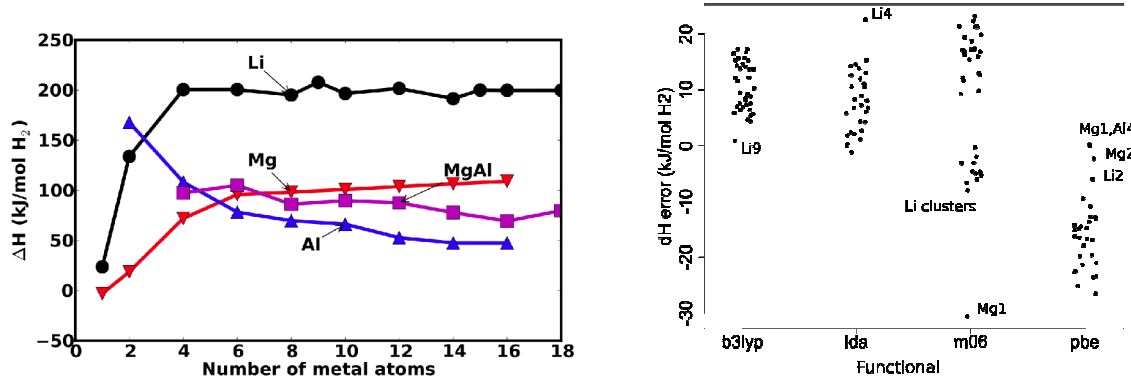


**Figure 10 (left).** Dependence of  $\Delta H$  on size, as calculated by diffusion Monte Carlo.

**Figure 11 (right).**  $\Delta H(\text{DFT}) - \Delta H(\text{DMC})$  for various DFT functionals. DMC agrees with high-level CCSD(T) results within 1 – 2 kJ/mol. The scatter in the  $x$  direction is to allow the reader to see all the points.

#### **TASK 2.4 PROJECT MANAGEMENT**

Biweekly conference calls among team members are continuing. A visit to UMSL by Mark Allendorf to present a seminar in spring 2011 is planned.

#### *PLANS FOR NEXT QUARTER:*

#### **Task 4: Tunable Thermodynamics and Kinetics for Hydrogen Storage: Nanoparticle Synthesis using Ordered Polymer Templates**

##### *Subtask 4.1 – Nanoparticle synthesis*

- Synthesize  $\text{MgH}_2$ -infiltrated MOFs using solution-based and melt-infiltration methods

##### *Subtask 4.2 – Hydrogen sorption measurements and kinetics*

- Complete and submit journal article describing  $\text{LiH}$  and  $\text{MgH}_2$  infiltrated MOFs
- Complete investigation of  $\text{NaAlH}_4@\text{Cu-BTC}$  decomposition and submit journal article.

##### *Subtask 4.3 – Theoretical Modeling for Rational Design of Particles*

- Complete Mg-Al-H cluster phase diagram (UMSL+MIT).

- Complete and submit journal article describing LiH QMC calculations

*Subtask 4.4 – Project Management*

Biweekly project conference calls

### **Publications and presentations**

Xiangfeng Liu, David Peaslee, Christopher Z. Jost, Eric H. Majzoub, Theodore F. Baumann  
“Phase diagram of nano-cluster NaAlH<sub>4</sub> from first-principles DFT,” submitted to *J. Phys. Chem. C*.

Raghu Bhakta, Richard Behrens, Aaron Highley, Sean Maharrey, Deneille Wiese-Smith, Benjamin Jacobs, Mark Allendorf, Eric Majzoub, X. Liu, D. Peaslee, Lucas Wagner, Jeffrey Grossman “Investigation of metal hydride nanoparticles templated in metal-organic frameworks,” presented at *Nano and Surface Science Approaches to Production and Storage of Hydrogen*,” 14-19 November 2010, Noordwijkerhout, The Netherlands

### ***TASK 5– COLLABORATIVE WEBSITE SUPPORT (STORAGE CENTERS & PROJECTS SHAREPOINT)***

Authors: Jennifer Rodriguez and Lynde Farhat

At the request of DOE, Sandia National Laboratories developed the Storage Centers & Projects QuickPlace in May 2005 for the purpose of sharing information in a secure environment among Hydrogen Storage colleagues and partners. The folders maintained within the website provide dated records of documents posted by various participants of the group. We will continue to maintain the membership list as approved by DOE and to provide posting services upon request for the restricted member private rooms: (1) DOE Hydrogen Storage (default all), (2) Center Leads and (3) SSAWG. We will continue to back up data of the website to provide a solution if information is accidentally deleted in the future.

Jennifer Rodriguez ([jenrodr@sandia.gov](mailto:jenrodr@sandia.gov)) maintains the website and membership list, acts as webmaster between SharePoint Administrators (technical support group) and the DOE Hydrogen Storage Program SharePoint members; providing posting services upon request. Lynde Farhat ([lfarhat@sandia.gov](mailto:lfarhat@sandia.gov)) is the point of contact for DOE and room managers for membership authorizations, training and any other concerns.

<http://h2-storage.net>

### ***(FY10 AOP—TASK 2) DEVELOP GENERALIZED METHODS AND PROCEDURES TO INVESTIGATE REACTIVITY PROPERTIES OF HYDROGEN STORAGE MATERIALS (PHASE II)***

Principal Investigator: Daniel E. Dedrick

The work planned under this task was competitively selected under DOE solicitation #DE-PS36-06GO96012F. The primary focus of this program is to develop generalized methods and procedures required to quantify the reactivity properties of hydrogen storage materials to enable the design, handling and operation of solids-based hydrogen storage systems. We are performing the experimental and modeling/simulation efforts that are required to understand chemical and physical processes during accident scenarios. Ultimately, this effort identifies and develops hazard mitigation strategies, and provides the technical basis that is required for eventual codes and standards development.

The project is organized into three subtasks:

- Subtask 2.1 Quantify contamination chemical processes and hazards (Phase I)
- Subtask 2.2 Predict chemical reactions and hazards during accident scenarios (Phase II)
- Subtask 2.3 Identify and demonstrate hazard mitigation strategies (Phase II)

### ***SUBTASK 2.3 Identify and demonstrate hazard mitigation strategies***

Task contributors: Joe Pratt, Craig Reeder, Joseph Cordaro, George Sartor

*Summary of accomplishments in Q1 of FY11:*

Finished the reactivity testing of copolymer polystyrene-divinylbenzene (ps-dvb) formulation, revealing the promise of polymer-based composites, and started work on new formulations to improve stability and functionality. Continued collaboration with United Technologies Research Center (UTRC) on testing the SNL-developed materials in applied conditions.

*Description:*

Mechanical testing of the sodium alanate with copolymer polystyrene-divinylbenzene (ps-dvb) composite material was finalized in this quarter. Results (reported in Ref. 1) revealed that while the composite showed promise in inhibiting the exothermic reaction of sodium alanate when exposed to air, the mitigating effect was not sustainable after repeated hydrogen charge/discharge cycling. The results also showed that, for the uncycled material, both hydrogen capacity and mitigating effect depended on the amount of crosslinking between polymer chains: more crosslinking reduced the hydrogen capacity but had better mitigating properties. Overall, the study on the sodium alanate with ps-dvb composite proved the concept of using a polymer additive to mitigate oxidation exothermicity while showing limitations of the current formulation, giving a path forward for the remainder of the project.

Therefore, this quarter attention turned to finding a new polymer composite that has mitigating properties while also being robust enough to undergo repeated hydrogen charge/discharge cycling. To see if a polystyrene-based polymer is feasible, we tested the thermal stability of polystyrene under conditions similar to the cycling of a storage tank. The results implied that the polystyrene backbone is sufficiently stable toward thermal degradation at these temperatures. Therefore, we feel confident that we can continue using a similar polymer backbone for synthesizing derivative polymers. New target materials based on polystyrene-like materials but incorporating siloxane moieties, were investigated in terms of synthesis technique and theoretical mitigating performance.

## **Publications and presentations**

1. Daniel E. Dedrick, Joseph G. Cordaro, Michael P. Kanouff, Craig L. Reeder, Joseph, W. Pratt, and Y. F. Khalil, “Mitigation Technologies for Hydrogen Storage Systems based on Reactive Solids,” presented at AIChE Annual Meeting, Salt Lake City, UT, Nov. 8-12, 2010.
2. Craig L. Reeder, Joseph W. Pratt, Joseph G. Cordaro, Michael P. Kanouff, Robert W. Bradshaw, and Daniel E. Dedrick, “Composite Materials for Solid-State Hydrogen Storage,” SAND Report 2010-4841P, 2010.